Micro- and Macrorheological Properties of Actin Networks Effectively Cross-Linked by Depletion Forces

R. Tharmann, M. M. A. E. Claessens, and A. R. Bausch
E22 Lehrstuhl für Biophysik, Technische Universität München, 85747 Garching, Germany

ABSTRACT The structure and rheology of cytoskeletal networks are regulated by actin binding proteins. Aside from these specific interactions, depletion forces can also alter the properties of cytoskeletal networks. Here we demonstrate that the addition of poly(ethylene glycol) (PEG) as a depletion agent results not only in severe structural changes, but also in alterations in mechanical properties of actin solutions. In the plateau of the elastic modulus two regimes can be distinguished by micro and macrorheological methods. In the first, the elastic modulus increases only slightly with increasing depletion agent, whereas above a critical concentration c^*, a strong increase of $c_{PEG6k}^{3.5}$ is observed in a distinct second regime. Microrheological data and electron microscopy images show a homogenous network of actin filaments in the first regime, whereas at higher PEG concentrations a network of actin bundles is observed. The concentration dependence of the plateau modulus G_0, the shift in entanglement time τ_e, and the nonlinear response indicate that below c^* the network becomes effectively cross-linked, whereas above c^* $G_0(c_{PEG6k})$ is primarily determined by the network of bundles that exhibits a linearly increasing bundle thickness.

INTRODUCTION

The unique mechanical properties of living cells are determined by the cytoskeleton, which is a dynamically organized complex, composite polymer network. Its predominant macromolecular constituent, F-actin, has been used extensively as an in vitro system to understand the physical principles of cytoskeletal rheology (1–4). In vivo, the microstructure of actin networks is regulated by numerous actin-binding proteins (ABPs). One major class of ABPs that determines the structure and thus mechanical properties of the networks are cross-linking proteins such as α-actinin and filamin. These proteins alter the structure and rheology of actin networks in a concentration-dependent manner, and it has been suggested that a tight control of cross-linker-mediated phase behavior is essential for cellular function (5,6). Nevertheless, cytoskeletal networks are affected not only by specific ABPs, but also by nonspecific means such as geometrical confinement and depletion forces exerted by surrounding small proteins or molecules present in the cytosol (7–10). The origin of the depletion force occurs quite generally in binary colloidal suspensions: when two larger particles approach to within a distance smaller than the diameter of the smaller colloidal particles, the overall configurational entropy is increased by excluding the latter from this region. Consequently, the depletion of the smaller particles results in an effective osmotic pressure and leads to an effective attraction between the larger colloidal species (8,11). The presence of a high concentration of small molecules in living cells is thought to affect the rate of biochemical reactions and even protein folding, which has been discussed extensively in the literature as molecular crowding (8,12,13). It has been shown by static light scattering, electron microscopy (EM), and fluorescence microscopy that, above a critical concentration, adding a typical depletion agent like poly(ethylene glycol) (PEG) to actin solutions results in bundling of filaments (14–16). The observed structural rearrangements of the networks are reminiscent of the structural changes induced by a high concentration of specific cross-linkers (17). However, for systems consisting of different cross-linker types, different structural transitions have been predicted. Although for depletion forces a direct crossover from an isotropic to a purely bundled phase is predicted, mixed phases should occur for specific cross-linkers depending on the binding energies (5,18).

Here, we show that concomitant with depletion-force-induced structural changes, the rheological behavior of in vitro actin networks changes dramatically. Depletion forces were induced by adding poly(ethylene glycol) to entangled actin solutions. Two viscoelastic regimes can be clearly distinguished: at low weight fractions of PEG, the elastic modulus increases only slightly with increasing depletion force. For concentrations of PEG higher than a critical concentration c^*, however, G' becomes strongly dependent on the concentration of the depletion agent. Electron microscopy allows us to relate the viscoelastic response of the network to structural changes: at low PEG6k concentrations, an isotropic disordered network dominates the viscoelastic response, whereas at concentrations above c^*, the response is determined by the presence of actin bundles.

MATERIALS AND METHODS

Actin was prepared from rabbit skeletal muscle according to Spudich and Watt (19) and stored in lyophilized form at −21°C. For measurements, the lyophilized actin was dissolved in water and dialyzed against fresh G-buffer (2 mM Tris, 0.2 mM adenosine triphosphate, 0.2 mM $CaCl_2$, 0.2 mM

Submitted July 19, 2005, and accepted for publication December 28, 2005.

Address reprint requests to Andreas R. Bausch, Lehrstuhl Für Biophysik E22, Technische Universität München, James Frank Str. 1, 85747 Garching, Germany. Tel.: 49-89-2891-2480; Fax: 49-89-2891-2469; E-mail: abausch@ph.tum.de.

0006-3495/06/04/2622/06 $2.00

doi: 10.1529/biophysj.105.070458

dithiothreitol, 0.005% NaN_3) at 4°C. The G-actin solution was centrifuged at 48,000 rpm and sterile-filtrated to minimize the fraction of residual actin-binding proteins. The monomeric actin was kept at 4°C for a maximum of 10 days. Polymerization was initiated by adding 1/10 of the sample volume of 10-fold concentrated F-buffer containing 20 mM Tris (pH 7.5), 2 mM $CaCl_2$, 1 M KCl, 20 mM $MgCl_2$, 2 mM dithiothreitol, and 5 mM adenosine triphosphate. Gelsolin was prepared from bovine plasma serum (20) and stored dissolved in G-buffer at −80°C. To adjust the mean length of actin filaments to 21 μm, gelsolin was added to the sample in the molar ratio of actin to gelsolin $r_{A/G} = 7770$ before initiating polymerization (21). All measurements were made at room temperature, 21°C. Poly(ethylene glycol) with a molecular mass of 6000 Da (PEG6k) and an approximate radius of gyration of 2 nm (Merck, Darmstadt, Germany) was diluted in millipore water (40% w/w) and added before the polymerization. Samples were gently mixed with pipettes with a cut-off tip. Polymerization assays by fluorescent spectrometry of 7-Chloro-nitrobenzo-2-oxa-1,3-diazole-labeled actin showed that the presence of PEG did not significantly affect the polymerization kinetics (22). The samples for transmission EM (TEM) (Philips EM 400T, New York, NY) were absorbed for 60 s to glow-discharged carbon-coated formvar films on copper grids that were washed in a drop of distilled water for 60 s before the negative staining (60 s) with 0.8% uranyl acetate. Excess liquid was drained with filter paper to the edge of the grid, which was then permitted to air dry. The bundle thickness was measured by determining a line profile perpendicular to the bundle. The intensity distribution was fitted with a Gaussian function and the width was determined.

The local elasticity of the network was probed by observing embedded negatively charged carboxylated latex beads (Interfacial Dynamics, Portland OR) with a 32× objective on an Axiovert 10 (Zeiss, Stuttgart, Germany). It has been shown that this particle surface has a negligible effect on the determination of the local elastic plateau modulus G_0 of actin networks (23). Images were captured at a frame rate of 36 ms/image with a charge-coupled device camera (Hamamatsu, Herrsching, Germany) and stored directly on hard disk. Image storage and analysis were done with the image processing software OpenBox (24). At long times, the mean-square displacement (MSD) $\langle \Delta x^2(\infty) \rangle$ of these particles exhibits a plateau that is used to extract the local elastic modulus G_0 of the network using $\langle \Delta x^2(\infty) \rangle = k_B T/(\pi G_0 a)$, where a is the particle radius (0.25 μm) (25,26).

The bulk rheological measurements in the linear response regime were performed with a magnetically driven rotating-disc rheometer (27). A sample volume of 400 μl was covered with a phospholipid monolayer (dimystriolphosphatidylcholine dissolved in chloroform) to prevent denaturation of actin at the air-water interface. G-actin polymerization was induced by adding 10-fold F-buffer and after 2 min of gentle mixing the polymerizing actin was transferred to the sample cuvette and the lipid layer was spread on the surface. After evaporation of the solvent of the lipids (2 min), the PEG6k was added with an injection below the lipid film in the sample volume. The rotating disc was placed onto the sample and the cuvette was covered with a glass slide to eliminate any evaporation effects. All rheological experiments were performed after 2 h of polymerization at room temperature. We detected the frequency dependent moduli $G'(f)$ and $G''(f)$ in a frequency range $f = 1$ Hz–1 mHz for all samples studied. The moduli of pure PEG solutions were negligible as they are over the whole frequency regime more than two orders of magnitude below the values measured for the composite actin-PEG networks.

To determine the nonlinear behavior of the networks, the sample is sheared continuously with a constant shear rate of 12.5%/s. These measurements were done with a commercially available rheometer (Physica, Anton Paar, Graz, Austria). The samples were measured in plate-plate geometry ($r = 25$ mm) with a gap size of 160 μm and a sample volume of 517 μl.

RESULTS AND DISCUSSION

The addition of PEG6k to the actin solution results in distinct changes in network structure and morphology. EM images show that below a critical PEG6k concentration c^*, actin filaments are organized as an isotropically disordered network (Fig.1, *a* and *b*). In this low PEG concentration regime, the appearance of actin bundles is rare; bundle formation starts at c^* (Fig. 1, *c* and *d*). As soon as bundles begin to form in the network, hardly any single filaments remain, which is consistent with previous observations using light microscopy and static light scattering (14–16). These findings reaffirm that here the isotropic network and bundled phases are noncoexistent in thermodynamic equilibrium. With increasing c_{PEG6k}, the cylindrical-appearing actin bundles grow

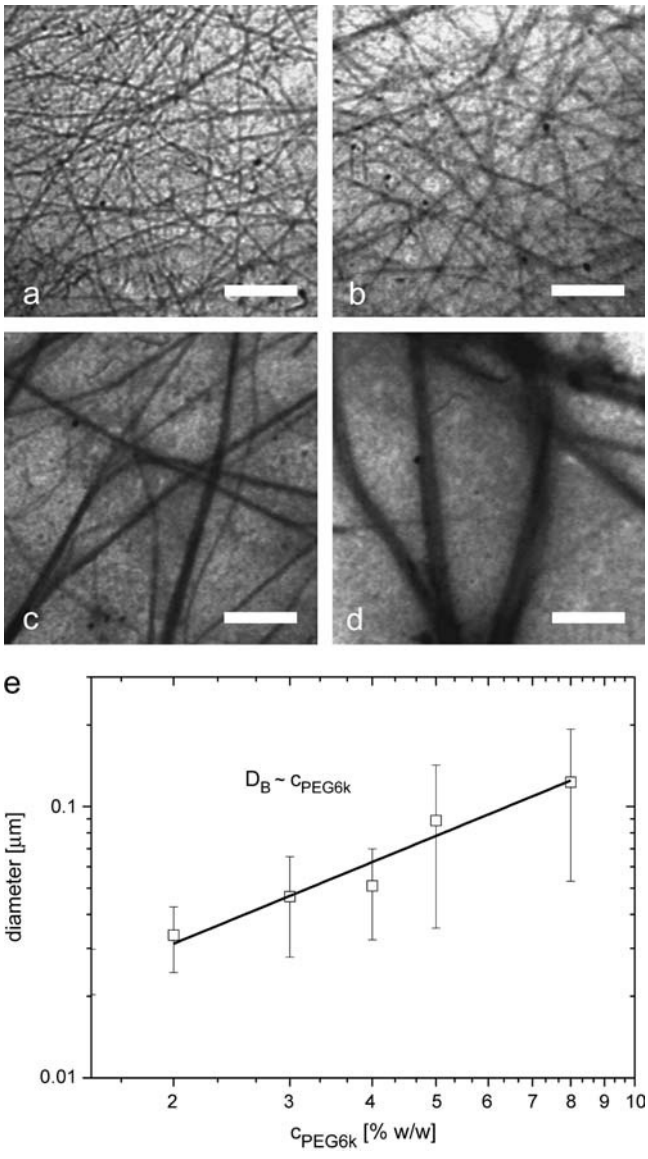

FIGURE 1 Electron microscopy pictures of composite F-Actin/PEG6k solution at different PEG concentrations ($c_{actin} = 9.5$ μM) (*a*) without any PEG and (*b–d*) with the addition of 1.5% w/w (*b*), 4% w/w (*c*), and 8% w/w (*d*) PEG6k (scale bar, 0.5 μm). (*e*) Increasing diameter of bundles determined by image analysis of the TEM pictures. Below c^*, no bundles where observed, whereas above c^*, the diameter of the bundles increases linearly (*solid line*) with the PEG6k concentration ($c_{actin} = 9.5$ μM).

linearly in diameter (Fig. 1 *e*) and the distance between the bundles increases. At yet higher concentrations of PEG (>8%), complete demixing of the solution is observed. The network structure changes dramatically above c^*, but even before bundling takes place smaller modifications in network properties are expected. To quantify the microstructure and rheology of the actin networks below c^*, the thermal motion of micrometer-sized colloids embedded in the network were analyzed (Fig. 2 *a*). Above c^*, the colloidal probe particles get trapped in the bundles and no analysis of their motion is possible. The same behavior is observed for PEG-covered beads where protein adsorption is reported to be minimized. The beads that are not trapped move through relatively large anisotropic pores and their MSD contains only information about the viscosity of the surrounding aqueous solution. Below c^*, the addition of PEG6k results in an increase of G_0 (Fig. 2 *a*, *inset*), whereas the relative width of the local MSD distribution stays nearly constant in this regime. Considering that the mean mesh size is constant (it only depends on the concentration of filaments), increases of the moduli cannot be attributed to changes of mesh size in an isotropic homogeneous network.

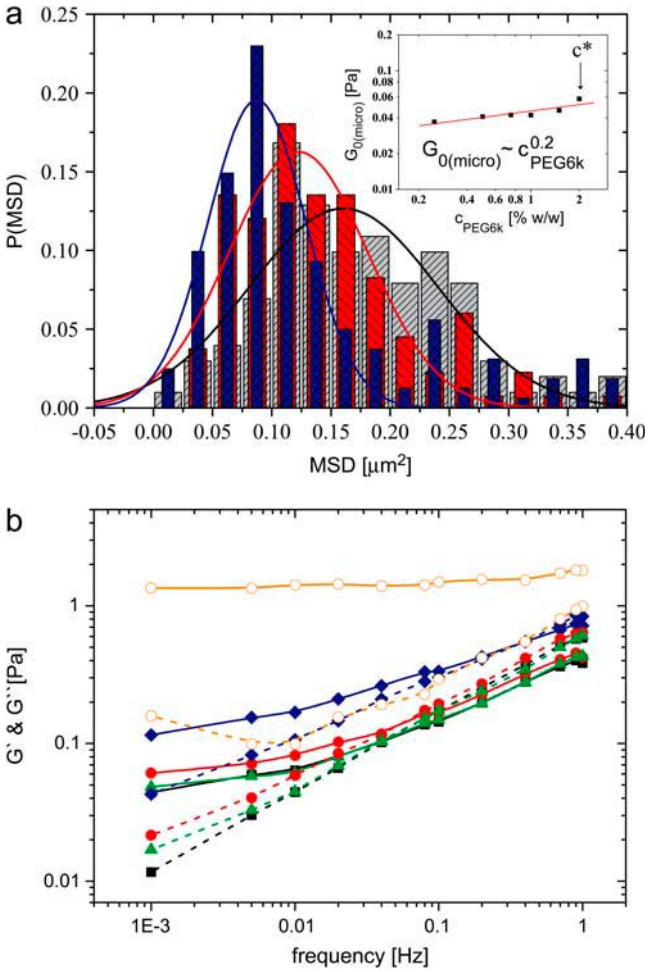

FIGURE 2 (*a*) Histogram of the local mean-square displacements of colloidal probe particles embedded in the actin network. Gray bars represent pure actin, red bars actin with addition of 1% w/w PEG, and blue bars actin with 2% w/w PEG. The center of the Gaussian fit (*solid lines*) can be used to calculate the plateau modulus at low frequencies as seen in the inset. Counts of beads were normalized by the maximal number of beads used for the distribution. (*b*) Frequency behavior of the moduli G' (*solid lines*) and G'' (*dashed lines*) for actin 9.5 μm (*black squares*), 0.6% w/w PEG6k (*red circles*), 1.25% w/w PEG6k (*green triangles*), 1.9% w/w PEG6k (*blue diamonds*), and 5% w/w PEG6k (*orange open circles*).

Concomitant with the observed local mechanical changes induced by increasing PEG concentration, the macroscopic viscoelastic properties of the network are expected to alter. Increasing the amounts of depletion agent increases the storage and loss moduli G' and G'' over the entire frequency range probed (Fig. 2 *b*). The absolute values of the plateau storage modulus as a function of PEG concentration are in excellent agreement with the mean values obtained from microrheology. With increasing elastic modulus, the frequency dependence of G' and G'' becomes less pronounced. Simultaneously, the entanglement crossover time τ_e is shifted to higher frequencies, which implies that single-filament fluctuations are hindered. At a c_{PEG6k} of 5% w/w the elastic modulus G' is nearly constant over the whole frequency range and τ_e is shifted outside the probed frequency range. Plotting the plateau modulus G_0 at a frequency of 5 mHz against the depletion agent concentration (c_{PEG6k}) (Fig. 3), the two regimes separated by c^* can easily be distinguished. From the rheology data we obtain $c^* \approx 2\%$ w/w for $c_{actin} = 9.5\ \mu$M, which is somewhat lower than the 4–8% reported by others under similar conditions (14,16). The variation in values of c^* can probably be attributed to differences in the actin preparation and sensitivity of the method for the appearance of bundles.

In the regime below c^* we observe a small but significant increase of $G_0 \propto c_{PEG6k}^{0.2\pm0.1}$, consistent with the microrheological findings. The increase in the regime below c^* and the shift in τ_e can be explained by a continuous change from a regime where the entanglements, and thus the tube deformations, dominate the elastic response to a regime where actin filaments are gradually pinned together and thus the force exerted on single filaments dominates the network. Forces exerted by depletion agents are homogeneous throughout the network, which implies that actin filaments are gradually pinned together more strongly with increasing PEG concentration—an increasingly stronger attraction corresponds to a deeper secondary minimum in the total interaction potential (16). Changing the steepness of the minimum of the interaction potential results in increasingly effective cross-links between the filaments and, as a result, the network behaves as if it were isotropically cross-linked. Thus, the substantially lower longitudinal thermal compliance of the filaments increasingly dominates the mechanical response of the network. This hypothesis agrees with the dependence of G_0 on c_{actin}; although G_0 scales as $G_0 \propto c_{actin}^{7/5}$ in entangled networks (1), a scaling of $G_0 \propto c_{actin}^{11/5}$ is reported for affine deformed cross-linked networks (28). Below c^*, $G_0(c_{PEG6k})$ can only

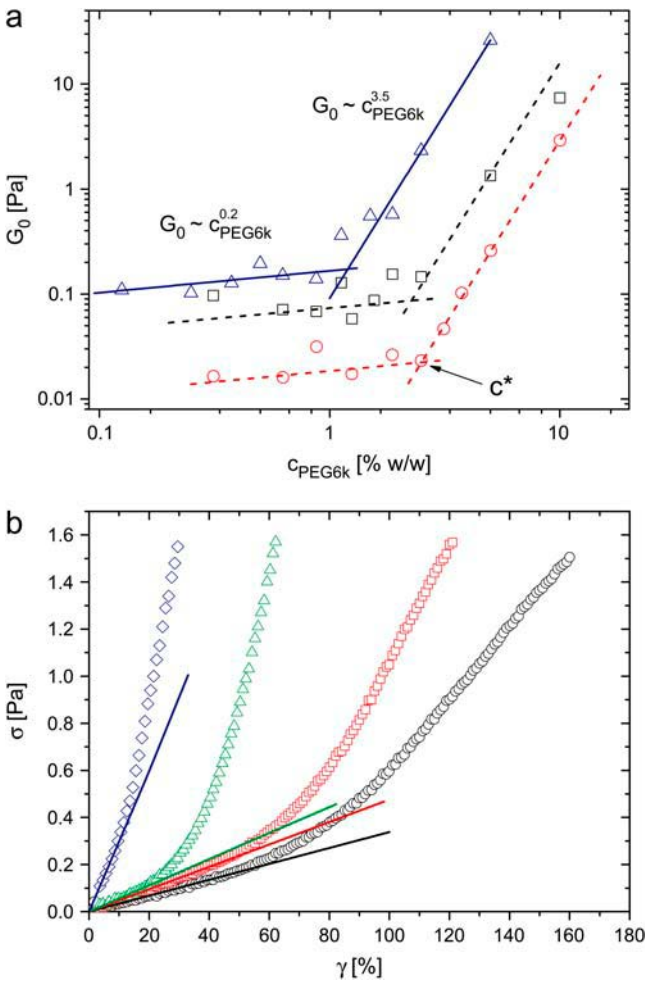

FIGURE 3 (*a*) Macrorheological modulus G_0 as a function of c_{PEG6k} taken from the frequency spectra at 5 mHz. In the concentration dependence of the moduli two regimes can be distinguished: Below c^* we find a small increase of the moduli $G_0 \propto c_{PEG6k}^{0.2\pm0.1}$, whereas above c^* a steep increase is observable: $G_0 \propto c_{PEG6k}^{3.5\pm0.6}$. The actin concentrations are 4.75 μM (*circles*), 9.5 μM (*squares*), and 14.3 μM (*triangles*). The solid line shows a best fit to the experimental data (14.3 μM actin). The dotted lines below c^* are obtained by using the scaling for cross-linked networks $G_0 \propto c_{actin}^{11/5}$ with constant prefactor. Above c^* the dotted lines are obtained by renormalizing the data by c^* and using the observed scaling for cross-linked bundled networks $G_0 \propto c_{actin}^{5/2}$ with constant prefactor. (*b*) The nonlinear regime was probed by shearing the sample at a defined shear rate of 12.5%/s. Initially, the stress increases linearly with the strain, and above a well defined strain a nonlinear stiffening response is observed: actin 9.5 μM (*circles*), 1% w/w PEG6k (*squares*), 1.5% w/w PEG6k (*triangles*), and 2% w/w PEG6k (*diamonds*). The increase in the slope $\delta\sigma/\delta\gamma$ of the linear response regime corresponds to the observed increase $G_0 \sim c_{PEG6k}^{0.2\pm0.1}$ obtained from the macro- and microrheological measurements.

be fitted using one single prefactor for all actin concentrations when it is assumed that $G_0 \propto c_{actin}^{11/5}$ and the mesh size ξ is smaller than the length between cross-links L_c (Fig. 3)

To underline our hypothesis that the attraction between the filaments is becoming stronger with increasing depletion forces, measurements to probe the onset of the nonlinear regime were performed. A strong prediction of the model we have used to fit $G_0(c_{PEG6k}, c_{actin})$ is that with increasing cross-link density the nonlinear response regime starts at decreasingly smaller deformations. To overcome difficulties in determining the nonlinear response of networks, a small oscillatory stress can be superposed on top of a constant applied stress (3,29). However, this technique is only applicable to networks for which the viscous response during the measurement can be neglected, which is not the case for entangled networks. The response of entangled and weakly cross-linked actin networks will depend crucially on the timescale at which the network is probed (30). To eliminate possible time effects due to viscous flow we increased the strain at constant shear rate and recorded the response of the sample. At low shear rate only small shear stiffening is observed, whereas for shear rates above 0.125^{-1}, the response is independent of the shear rate (C. Semmrich and A. R. Bausch, unpublished).

When deforming the composite networks below c^* at a constant shear rate of 0.125 s^{-1}, the onset of nonlinear elasticity decreases almost linearly ($\sim 25\%/c_{PEG6k}$) with increasing concentration of depletion agent (Fig. 3 *b*). This suggests that increasing attractions between the filaments is equivalent to increasing cross-linker density. The increase in the initial slope $\delta\sigma/\delta\gamma$ of the linear response regime corresponds to the observed increase $G_0 \sim c_{PEG6k}^{0.2}$ obtained from the macro- and microrheological measurements. In contrast to reports in the literature (3), a strain hardening of the entangled actin network was observed in our measurements (30,32).

At c^*, interfilament attractions become strong enough to overcome entropic contributions of single-filament fluctuations (and mixing), and thus bundling becomes energetically favorable and a phase transition is observed (5,16). Above c^*, the appearance of a network of bundles results in a much more pronounced increase of $G_0 \propto c_{PEG6k}^{3.5\pm0.6}$ for all actin concentrations studied (Fig. 3 *b*). The concentration c^*, and thus the magnitude of the depletion forces needed to induce the structural transition, depends on c_{actin}. Theoretical predictions for c^* depend on the microscopic interaction potential, taking into account explicitly not only the magnitude of the depletion force but also the standard Derjaguin-Landau-Verwey-Overbeek potential between the charged filaments (16,18,33).

The moduli are determined by both the concentration and the mechanical properties of the bundles. Generally it is assumed that the network can be decomposed into statistically identical elastic unit cells of linear dimensions equal to the mesh size ξ, as is the case for foams and other cellular solids, and that the macroscopic response is simply the upscaled response of such a cell. The elastic response can be estimated by simple arguments and depends on whether the cell response is dominated by bending (34) or stretching (35) modes.

At constant actin concentration, bundling of n filaments results in an increase of the mesh size $\xi \propto (n/c_a)^{1/2}$. Concurrently, if one assumes tight interfilament coupling, the persistence length l_p of a bundle with a diameter D_B will

increase as $l_p \propto D_B^4$ in accordance with theoretical predictions for homogeneous elastic rods (36,37, and M. M. A. E. Claessens and A. R. Bausch, unpublished). Because the area of the bundle scales linearly with the number of filaments ($A \sim n \sim D_B^2$), the persistence length is quadratic with the number of filaments ($l_p \propto n^2$).

Interestingly, in the bending-dominated case, the effect of bundling is predicted to cancel out of the expression for the shear modulus, since the increase in stiffness of the bundles is exactly balanced by the increase in mesh size. In the stretching-dominated case, a stiffening with an increasing number of filaments in the bundles is predicted when $L_c = \xi$:

$$G_0 \propto \frac{l_p^2}{\xi^5} \propto n^{\frac{3}{5}}. \quad (1)$$

To obtain the experimental observed dependence of $G_0 \propto c_{PEG6k}^{3.5}$, the number of filaments in the bundle should scale as $n \propto c_{PEG6k}^{2.3}$, and therefore the bundle diameter ($D_B = 2r$) should scale with the PEG6k concentration $D_B \propto c_{PEG6k}^{1.2}$. Indeed, by measuring the bundle thickness in the TEM pictures, a nearly linear increase of the mean bundle thickness can be observed (Fig. 1 *e*). The increase of $G_0(c_{PEG6k})$ for the different actin concentrations can again be fitted using one prefactor, but now the data has to be rescaled at the onset of the bundling regime, c^*; the plateau modulus now scales as $G_0 \propto c_{actin}^{5/2}$, consistent with Eq. 1 (Fig. 3 *a*).

One should be cautious, however, not to hastily conclude that the detailed mechanism of the elastic response in this regime is therefore understood. It is important to realize that, as a consequence of the quadratic dependence of the persistence length on the number of filaments in the bundles already, bundles of 10 filaments have persistence lengths in the millimeter range. It is hard to imagine how a linear response is still dominated by entropic contribution with such stiff rods. As was recently convincingly demonstrated for two-dimensional random fiber networks (39), the simple cell model is not applicable to elastic rod networks, so that the proper explanation for the observed increase in elasticity may be somewhat more complicated. Only mesoscopic simulations will enable us to further understand the underlying physics (39–41).

A phase transition from an isotropically cross-linked network to a microgel and finally to a network of bundles has been observed in α-actinin cross-linked networks (6). In contrast to these specifically cross-linked networks the unspecifically acting depletion forces induce a direct transition of the isotropically cross-linked network to a pure network of bundles; microgel formation was not observed. The rheological properties reveal structural changes and changes in the effective interaction inside each phase. The observed dependence of $G_0(c_{PEG6k})$ above c^* is much stronger for the depletion forces than observed for short rigid cross-linkers like scruin, where the moduli scaled with $G_0 \propto c_{CL}^2$ (28,29). This can be attributed to the fact that for depletion forces a pure bundle phase is observed, whereas for scruin a mixed phase of bundles and isotropic network was observed. This suggests that the scaling of the moduli with the cross-linking molecules gives a measure for the bundle effectiveness of the cross-linking molecule. The bundle effectiveness of the cross-linking agent will depend on the geometry of the binding domains and the interaction energies of the cross-linker. These determine whether a purely bundled network or an isotropic cross-linked network mixed with bundles or even a nematic phase is present (5). Specific cross-linkers can only bind locally, and the bundling is limited by the discrete cross-linker densities and their geometry. The continuously increasing homogenous attraction induced by depletion agents acts along the full filament length, and thus bundling is most effective. Interestingly, for networks cross-linked by specific cross-linkers such as α-actinin or scruin, no increase at low concentrations was observed and a strong increase of the moduli had already started at concentrations of $\sim 1\ \mu$M, which is a factor of $\sim 10^3$ less than that observed for the unspecific depletion forces.

The stability of the solution and the observed demixing above 8% PEG suggest that a finite equilibrium bundle size exists over a defined range of PEG concentrations. As the depletion attraction should increase with increasing bundle diameter, the equilibrium bundle size should be attributed to a repulsive interaction between the bundles. This repulsion may arise from interactions between bundles, which could be elastic and which are overcome at high PEG concentrations where the full demixing of the solution is observed (42). However, further investigations of this phenomenon are necessary to fully understand the observed phase behavior.

CONCLUSION

A structural and mechanical phase transition between an isotropically cross-linked and a purely bundled phase is observed at a critical depletion force. Within each phase the network, structure is changing as a function of the concentration of the depletion agent. The observed viscoelastic behavior of actin networks in the presence of depletion forces suggests that depletion forces act as effective cross-linkers in vivo, altering the network structure and mechanics dramatically. In cells, ~18–27% of the volume consists of globular proteins, and thus, depletion forces will be strong enough to severely alter cytoskeletal structure and mechanics (10). In the crowded environment of cells, low concentrations of specific cross-linkers might thus be acting in an already prearranged network, structuring and thereby fortifying it. For further elucidation of the function of specific cross-linkers in in vitro systems it will be important to consider specific cross-linkers and depletion forces simultaneously.

We thank Monika Rusp for the actin preparation. We are especially grateful for many fruitful discussions with Klaus Kroy, Erwin Frey, Claus Heussinger, and Mark Bathe.

This work was supported by the Deutsche Forschungsgemeinschaft (SFB413 C3). We gratefully acknowledge also the support of the Fonds der Chemischen Industrie.

REFERENCES

1. Hinner, B., M. Tempel, E. Sackmann, K. Kroy, and E. Frey. 1998. Entanglement, elasticity, and viscous relaxation of actin solutions. *Phys. Rev. Lett.* 81:2614–2617.
2. Gardel, M. L., M. T. Valentine, J. C. Crocker, A. R. Bausch, and D. A. Weitz. 2003. Microrheology of entangled F-actin solutions. *Phys. Rev. Lett.* 91:158302.
3. Gardel, M. L., J. H. Shin, F. C. MacKintosh, L. Mahadevan, P. Matsudaira, and D. A. Weitz. 2004. Elastic behavior of cross-linked and bundled actin networks. *Science.* 304:1301–1305.
4. Bausch, A. R., and K. Kroy. 2006. Cytoskeleton from the assembly line: a bottom-up approach to cell mechanics. *Nature Physics.* doi: 10.1038/nphys260.
5. Borukhov, L., R. F. Bruinsma, W. M. Gelbart, and A. J. Liu. 2005. Structural polymorphism of the cytoskeleton: a model of linker-assisted filament aggregation. *Proc. Natl. Acad. Sci. USA.* 102:3673–3678.
6. Tempel, M., G. Isenberg, and E. Sackmann. 1996. Temperature-induced sol-gel transition and microgel formation in alpha-actinin cross-linked actin networks: a rheological study. *Phys. Rev. E.* 54:1802–1810.
7. Classens, M. M. A. E., R. Tharmann, K. Kroy, and A. R. Bauch. 2006. Microstructure and viscoelasticity of confined semiflexible polymer networks. *Nature Physics.* doi: 10.1038/nphys241.
8. Madden, T. L., and J. Herzfeld. 1993. Crowding-induced organization of cytoskeletal elements. 1. Spontaneous demixing of cytosolic proteins and model filaments to form filament bundles. *Biophys. J.* 65: 1147–1154.
9. Madden, T. L., and J. Herzfeld. 1994. Crowding-induced organization of cytoskeletal elements. 2. Dissolution of spontaneously formed filament bundles by capping proteins. *J. Cell Biol.* 126:169–174.
10. Kulp, D. T., and J. Herzfeld. 1995. Crowding-induced organization of cytoskeletal elements. 3. Spontaneous bundling and sorting of self-assembled filaments with different flexibilities. *Biophys. Chem.* 57: 93–102.
11. Asakura, S., and F. Oosawa. 1954. On interaction between two bodies immersed in a solution of macromolecules. *J. Chem. Phys.* 22: 1255–1256.
12. Ellis, R. J. 2001. Macromolecular crowding: an important but neglected aspect of the intracellular environment. *Curr. Opin. Struct. Biol.* 11:114–119.
13. Herzfeld, J. 2004. Crowding-induced organization in cells: spontaneous alignment and sorting of filaments with physiological control points. *J. Mol. Recognit.* 17:376–381.
14. Suzuki, A., M. Yamazaki, and T. Ito. 1989. Osmoelastic coupling in biological structures: formation of parallel bundles of actin filaments in a crystalline-like structure caused by osmotic stress. *Biochemistry.* 28:6513–6518.
15. Suzuki, A., M. Yamazaki, and T. Ito. 1996. Polymorphism of F-actin assembly. 1. A quantitative phase diagram of F-actin. *Biochemistry.* 35:5238–5244.
16. Hosek, M., and J. X. Tang. 2004. Polymer-induced bundling of F actin and the depletion force. *Phys. Rev. E.* 69:051907.
17. Pelletier, O., E. Pokidysheva, L. S. Hirst, N. Bouxsein, Y. Li, and C. R. Safinya. 2003. Structure of actin cross-linked with alpha-actinin: a network of bundles. *Phys. Rev. Lett.* 91:148102.
18. Zilman, A. G., and S. A. Safran. 2003. Role of cross-links in bundle formation, phase separation and gelation of long filaments. *Europhys. Lett.* 63:139–145.
19. Spudich, J. A., and S. Watt. 1971. Regulation of rabbit skeletal muscle contraction. 1. Biochemical studies of interaction of tropomyosin-troponin complex with actin and proteolytic fragments of myosin. *J. Biol. Chem.* 246:4866–4871.
20. Cooper, J. A., J. Bryan, B. Schwab, C. Frieden, D. J. Loftus, and E. L. Elson. 1987. Microinjection of gelsolin into living cells. *J. Cell Biol.* 104:491–501.
21. Janmey, P. A., J. Peetermans, K. S. Zaner, T. P. Stossel, and T. Tanaka. 1986. Structure and mobility of actin filaments as measured by quasielastic light scattering, viscometry, and electron microscopy. *J. Biol. Chem.* 261:8357–8362.
22. Lindner, R. A., and G. B. Ralston. 1997. Macromolecular crowding: effects on actin polymerisation. *Biophys. Chem.* 66:57–66.
23. Valentine, M. T., Z. E. Perlman, M. L. Gardel, J. H. Shin, P. Matsudaira, T. J. Mitchison, and D. A. Weitz. 2004. Colloid surface chemistry critically affects multiple particle tracking measurements of biomaterials. *Biophys. J.* 86:4004–4014.
24. Schilling, J., E. Sackmann, and A. R. Bausch. 2004. Digital imaging processing for biophysical applications. *Rev. Sci. Instrum.* 75:2822–2827.
25. Valentine, M. T., P. D. Kaplan, D. Thota, J. C. Crocker, T. Gisler, R. K. Prud'homme, M. Beck, and D. A. Weitz. 2001. Investigating the microenvironments of inhomogeneous soft materials with multiple particle tracking. *Phys. Rev. E.* 6406:061506.
26. Wong, I. Y., M. L. Gardel, D. R. Reichman, E. R. Weeks, M. T. Valentine, A. R. Bausch, and D. A. Weitz. 2004. Anomalous diffusion probes microstructure dynamics of entangled F-actin networks. *Phys. Rev. Lett.* 92:178101.
27. Muller, O., H. E. Gaub, M. Barmann, and E. Sackmann. 1991. Viscoelastic moduli of sterically and chemically cross-linked actin networks in the dilute to semidilute regime: measurements by an oscillating disk rheometer. *Macromolecules.* 24:3111–3120.
28. Gardel, M. L., J. H. Shin, F. C. MacKintosh, L. Mahadevan, P. A. Matsudaira, and D. A. Weitz. 2004. Scaling of F-actin network rheology to probe single filament elasticity and dynamics. *Phys. Rev. Lett.* 93:188102.
29. Shin, J. H., M. L. Gardel, L. Mahadevan, P. Matsudaira, and D. A. Weitz. 2004. Relating microstructure to rheology of a bundled and cross-linked F-actin network in vitro. *Proc. Natl. Acad. Sci. USA.* 101:9636–9641.
30. Xu, J., Y. Tseng, and D. Wirtz. 2000. Strain hardening of actin filament networks. Regulation by the dynamic cross-linking protein α-actinin. *J. Biol. Chem.* 275:35886–35892.
31. Reference deleted in proof.
32. Janmey, P. A., S. Hvidt, J. Kas, D. Lerche, A. Maggs, E. Sackmann, M. Schliwa, and T. P. Stossel. 1994. The mechanical properties of actin gels: elastic modulus and filament motions. *J. Biol. Chem.* 269:32503–32513.
33. de Vries, R. 2001. Flexible polymer-induced condensation and bundle formation of DNA and F-actin filaments. *Biophys. J.* 80:1186–1194.
34. Kroy, K., and E. Frey. 1996. Force-extension relation and plateau modulus for wormlike chains. *Phys. Rev. Lett.* 77:306–309.
35. Mackintosh, F. C., J. Kas, and P. A. Janmey. 1995. Elasticity of semiflexible biopolymer networks. *Phys. Rev. Lett.* 75:4425–4428.
36. Shin, J. H., L. Mahadevan, P. T. So, and P. Matsudaira. 2004. Bending stiffness of a crystalline actin bundle. *J. Mol. Biol.* 337:255–261.
37. Landau, L. D., and E. M. Lifshitz. 1986. Theory of Elasticity. Pergamon, New York.
38. Reference deleted in proof.
39. Heussinger, C., and E. Frey. 2005. Stiff polymers, foams and fiber networks. *Phys. Rev. Lett.* 96:017802.
40. Wilhelm, J., and E. Frey. 2003. Elasticity of stiff polymer networks. *Phys. Rev. Lett.* 91:108103.
41. Head, D. A., A. J. Levine, and F. C. MacKintosh. 2003. Distinct regimes of elastic response and deformation modes of cross-linked cytoskeletal and semiflexible polymer networks. *Phys. Rev. E.* 68: 061907.
42. Henle, M. L., and P. A. Pincus. 2005. Equilibrium bundle size of rodlike polyelectrolytes with counterion-induced attractive interactions. *Phys. Rev. E.* 71:060801.